Characterizing the Seasonal Cycle of the Northern Australian Rainy Season

JOHN UEHLING

Department of Earth, Ocean and Atmospheric Science, and Center for Ocean-Atmospheric Prediction Studies, Florida State University, Tallahassee, Florida

VASUBANDHU MISRA

Department of Earth, Ocean and Atmospheric Science, and Center for Ocean-Atmospheric Prediction Studies, and Florida Climate Institute, Florida State University, Tallahassee, Florida

(Manuscript received 2 August 2019, in final form 16 July 2020)

ABSTRACT

In this paper we introduce an objective definition for the onset and the retreat of the northern Australian rainy season that overlaps significantly with the Australian monsoon season. We define onset and retreat dates of the northern Australian rainy season as being the first and the last day of the year when the daily rain rate exceeds and falls below the climatological annual mean rain rate, respectively. However, our definition of onset/demise is not as restrictive as the traditional monsoon season that seeks the arrival of the westerlies and the equatorward retreat of the trough at its onset and demise, respectively. As defined in this paper, the length of the rainy season is longer than the monsoon season and includes the pre- and post-monsoon rainfall. It is noted that an early or later onset date of the northern Australian rainy season is associated with a longer or shorter, wetter or drier, and colder or warmer season, respectively. Similar relationship is also observed with demise date variations, which are, however, weaker than the onset date variations. Furthermore, we find that the relationship of the northern Australian seasonal rainfall variations with ENSO variability becomes stronger when we account for variations in the length of the rainy season compared to the fixed (December–February) monsoon season length. We also find a significant linear trend over the time period of the analysis from 1901 to 2015 toward an increasing length of the northern Australian rainy season that influences the corresponding rising trend of seasonal rainfall anomalies.

KEYWORDS: Australia; Climate change; Climate variability; ENSO; Interannual variability; Tropical variability

1. Introduction

In this paper, we propose to introduce a large-scale rainfall index to define the northern Australian rainy season, akin to Noska and Misra (2016) for the Indian summer monsoon. It may be noted that we make a subtle distinction here between the northern Australian monsoon season and its rainy season. This is because in our proposed definition of the season we use only rainfall as the variable and do not take the winds into consideration. Therefore, the ''traditional'' definition of the monsoon season that warrants the arrival of the westerlies in northern Australia (e.g., Troup 1961; Nicholls et al. 1982; Holland 1986; Drosdowsky 1996; Cook and Heerdegen 2001; Lo and Wheeler 2007) is not necessarily met in our definition.

The Australian monsoon, also known as the Indo-Australian monsoon or the Asian–Australian monsoon, is a phenomenon where between the months of December and March, enhanced rainfall occurs over the northern region of the Australian continent (Troup 1961; McBride 1983, 1987; Nicholls 1984; Wang et al. 2003). During the austral summer months, west to northwesterly winds bring moist air originating over the warm waters of the Indo–west Pacific Ocean over northern Australia (Troup 1961; Murakami and Sumi 1982). Similarly, Holland (1986) defined the onset and demise of the Australian monsoon as the first and the last days of westerlies at 850 hPa over Darwin in northern Australia. In fact, Holland (1986) indicated significant intraseasonal and interannual variations in the onset, retreat, rainfall anomalies of the Australian

Corresponding author: Vasubandhu Misra, vmisra@fsu.edu

DOI: 10.1175/JCLI-D-19-0592.1

monsoon. These monsoon rains are extremely important for the Australian agricultural productivity and other related economic activity, especially given the aridity of Australia (Anwar et al. 2007; Qureshi et al. 2013).

A majority of the prior studies have focused on the Australian summer monsoon season. Nicholls et al. (1982) and Nicholls (1984) recognized however, that the rainy season starts earlier and lasts longer than the typical northern Australian monsoon season. Cook and Heerdegen (2001) have argued that the timing of many ecologically important processes is not determined by the evolution of the Australian monsoon but by what they term as extramonsoonal rainfall events. These events as they define are based on the probability of occurrence of the 10-day wet and dry events over northern Australia. Similarly, Lo and Wheeler (2007) highlight the importance of premonsoon rainfall in northern Australia and proposed a statistical forecast model to predict the onset of the early wet-season rainfall. In a related study, Smith et al. (2008) defined onset and demise of the wet season over northern Australia as the date when 15% and 85% of the seasonal total rainfall is accumulated, respectively. Such a definition, however, is limited to retrospective analysis of the season.

The overlap of the rainy season with the monsoon season in northern Australia is, however, significant. The strongest effects of the Australian monsoon are felt in the domain covered, approximately 10°–20°S, 120°–150°E, where the annual peak of the rainfall coincides with the monsoon season (Atkinson 1971; Davidson et al. 1983, 1984; Holland 1986). Numerous studies have been conducted about the seasonality of the Australian monsoon, with different indexes being developed using various methodologies (e.g., wind based, rainfall based) to determine the onset and the demise of the Australian monsoon (Troup 1961; Murakami and Sumi 1982; Nicholls et al. 1982; Davidson et al. 1983, 1984; Holland 1986). The readers are encouraged to see Lisonbee et al. (2020) for a very detailed comparison of these indices of the Australian monsoon/rainy season.

These previous studies were, however, all limited somewhat in the scope of their analysis. For example, indices that are developed based on data over a single station location like Darwin undermine the wider region of northern Australia that is impacted by the monsoon. In terms of real-time application, monitoring the onset/demise of the monsoon from such single station indices can become challenging when a false onsets/demise could be triggered by isolated weather events that are unconnected to the large-scale seasonal evolution of the monsoon. Furthermore, Lisonbee et al. (2020) indicate similar shortcomings and highlight the inadequacy of most current indices for adapting to real-time monitoring or prognostic applications. However, the advantages of an index for the northern Australian rainy season as defined in this paper are as follows: 1) it is based on single rainfall variable that is now observed more extensively, both from a wide and a relatively dense network of in situ rain gauge observations and remotely sensed satellite platforms that would be available for real time application; 2) it is less susceptible to false onset/demise as it is based on an area average over a large northern Australian monsoon domain (Fig. 1a); and 3) many sectors such as agriculture, public health, and tourism are affected by variations in the rainy season and therefore it is a worthwhile endeavor to monitor the season by such an index. Moreover, rainfall over northern Australia is available over a longer period than the upper-air observations, which becomes critical to

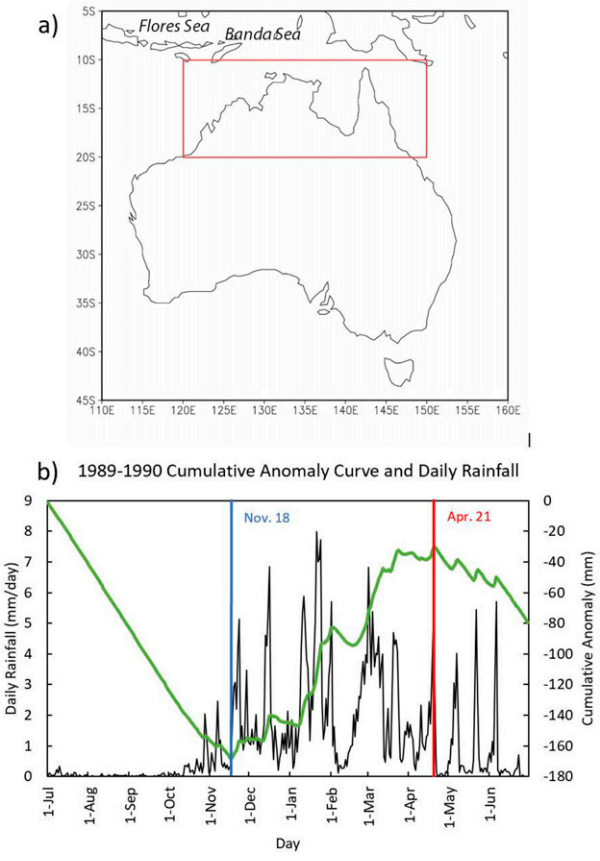

FIG. 1. (a) The continental region outlined by the red box is used to define the rainy season of northern Australia. (b) The time series of daily rainfall averaged over northern Australia (black line) overlaid with the corresponding cumulative anomaly curve (green line). The minimum in the cumulative anomaly curve is diagnosed as the onset date (indicated by blue line; 18 Nov 1989) and the maximum as the demise date (indicated by red line; 21 Apr 1990) of the Australian rainy season for the year 1989–90.

assess and diagnose the climate change signal. Furthermore, the consistency of such an index with the overall evolution of the monsoon and its variations will be presented in the paper to repose more confidence in the index and to show that it does overlap significantly with the Australian monsoon season. In addition, this study will show that the consideration for varying length of the northern Australian rainy season is important in gauging its teleconnections with ENSO.

The onset and the demise of the wet season are recognized to be spatially nonuniform processes (Tanaka 1994; Murakami and Matsumoto 1994; Misra et al. 2017). Nonetheless, large-scale indices offer a relatively simple metric to the seasonal variations of the wet season that display very rich temporal variations across many time scales. These large-scale indices are relatively less sensitive to the temporal variations of the density of observations and are therefore useful in robustly diagnosing the existence of any climate change signal. Moreover, as Misra et al. (2017) demonstrated in the case of the Indian summer monsoon, such large-scale indices of the rainy season can be further leveraged to anchor the definitions of local onset and demise of the season. In the next section we present the details of the datasets followed by the description of the methodology in section 3. The results are discussed in section 4 followed by final concluding remarks in section 5.

2. Datasets

The data used in this study were sourced from the Australian Bureau of Meteorology's rain gauge network across the Australian continent (http://www.bom.gov.au/climate/how/newproducts/IDCdrgrids.shtml; Grant 2012). The dataset is available on a 0.5° grid over the Australian landmass. The data range from 1 January 1900 through until 31 December 2015 for a total time period of 115 years of data. The rain gauge data were gridded using an optimized Barnes successive correction technique (Jones et al. 2009). There are, however, some limitations to this dataset, which include the sparseness of the rain gauge data in the outback and other rural areas that limits accuracy of the data (Grant 2012). But in our study, it should not be of a major concern due to the relatively denser observation network over the area of northern Australia (Grant 2012), which is the focus of this study (Fig. 1a). Furthermore, by using the area average of rainfall over the northern Australian domain (Fig. 1a) we make our index less sensitive to temporal variations in the density of the rain gauge observation network. Grant (2012) also points out that in regions with a high observational density, or where there are strong gradients, the data-smoothing technique applied to the data could potentially result in certain gridpoint values that differ from the rainfall amounts at the contributing stations. Grant (2012) further claims that the daily rainfall values have a root-mean-square error of 3.1 mm and a mean absolute error of 0.9 mm. The daily rainfall is nominally measured each day at 0900 local time.

Additionally, other atmospheric variables were also analyzed from the Climate Forecast System Reanalysis (CFSR; Saha et al. 2010), which has global atmospheric data dating back to 1979. The atmospheric reanalysis data valid at 0000 UTC were used to contrast the seasonal cycle of other kinematic and thermodynamic variables with rainfall over the evolution of the Australian rainy season. The SST dataset used in this study was also obtained from CFSR.

3. Methodology

The onset and demise of the northern Australian rainy season were diagnosed following Liebmann et al. (2007) and Noska and Misra (2016). The highlight of this methodology is one can objectively define the onset/demise of the rainy season to the day of the year. The daily rainfall is averaged over northern Australia (outlined in Fig. 1a). Many studies (e.g., Atkinson 1971; Davidson et al. 1983, 1984; Holland 1986; Kajikawa et al. 2010) indicate that the heaviest rainfall associated with the Australian monsoon occurs roughly over this domain outlined in Fig. 1a. A cumulative anomaly curve of the daily area averaged precipitation is then computed as

$$A_m(i) = \sum_{n=1}^{j} (\bar{r}_m(n) - \overline{\bar{r}}), \tag{1}$$

where $A_m(i)$ is the cumulative anomaly curve of the area averaged precipitation for day i of year m, $\bar{r}_m(n)$ is spatially averaged rainfall over northern Australia (Fig. 1a) for day n of year m, and $\overline{\bar{r}}$ is the area average, annual mean climatology of rainfall, which is given by

$$\overline{\bar{r}} = \frac{1}{MNK} \sum_{m=1}^{M} \sum_{n=1}^{N} \sum_{i=1}^{K} r(m,n,i), \tag{2}$$

where the summation over i is for area average by averaging over all K grid points over northern Australia, summation over n is averaging over all N days of the year for getting the annual mean, and the summation over m is over all M years (1901–2015) to obtain the climatology of the annual mean. It may be noted that in the summation, $n = 1$ and N in Eq. (1) is 1 September of a given year and 31 October of the following year, respectively. The minima and maxima in the $A_m(i)$ curve correspond to the onset and demise dates of the rainy

TABLE 1. Highlights of the Australian rainy season.

Feature	Value
Climatological length of the rainy season	115 days (standard deviation = 29.5 days)
Shortest season	31 days (year: 1901/02)
Longest season	191 days (year: 2010/11)
Climatological onset date of rainy season	7 Dec (standard deviation = 18 days)
Climatological demise date of rainy season	1 Apr (standard deviation = 19 days)
Earliest onset date of the rainy season	11 Feb 1905
Latest demise date of the rainy season	27 May 1968

season, respectively. This is illustrated with an example in Fig. 1b for the year 1989–90. The onset date as defined here is the first day of the year when the area averaged daily rainfall over northern Australia exceeds the corresponding annual mean climatology ($\overline{\overline{r}}$). In Fig. 1b, the onset date happens to be on 18 November 1989. Likewise, the demise date as defined here is the last day of the year when the area averaged rainfall over northern Australia falls below the corresponding annual mean climatology. In Fig. 1b, the demise date is diagnosed as 21 April 1990. The diagnosis of these dates is robust because it is based on 115 years of data, which provides for a good estimate of the annual mean climatology. Furthermore, area average over a large region like northern Australia avoids diagnosis of false onset and demise dates. These false onset/demise dates are often triggered by small-scale rain events that would be less impactful on the cumulative anomaly curve of the daily rainfall averaged over a large area like northern Australia.

4. Results

a. Linear trends in the evolution of the rainy season

The onset/demise dates of the northern Australian rainy season were computed for 113 years (1900/01 to 2014/15). The climatological seasonal length of the rainy season is 115 days with a standard deviation of 29.5 days (see Table 1). In the time series, the shortest season was only 31 days long (1901/02 season) and the longest season was 191 days long (2010/11 season). The climatological onset and demise date of the northern Australian rainy season is 7 December and 1 April, respectively. The standard deviation of the onset and the demise dates about their corresponding means are 18 and 19 days, respectively. The earliest and latest onset dates were 8 October 2010 and 26 January 1906, respectively. Similarly, the earliest and the latest retreat dates of the northern Australian rainy season occurred on 11 February 1905 and 27 May 1968, respectively.

The time series of the length (Fig. 2a), corresponding onset date (Fig. 2b), and retreat date (Fig. 2c) of the northern Australian rainy season clearly indicate strong linear trends whose slopes pass the Mann–Kendall statistical significance test at a 99% confidence interval (Hirsch and Slack 1984; Table 2). Table 2 also indicates the corresponding nonparametric Sen slope of these trends (Sen 1968). These figures and Table 2 suggest that length of the season is increasing at the rate of 0.34 days yr^{-1} (Fig. 2a), the onset date of the Northern Australian rainy season is occurring earlier at the rate of 0.18 days yr^{-1} (Fig. 2b), and the demise date is occurring later at the rate of 0.15 days yr^{-1} (Fig. 2c). On account of these changes to the evolution of the northern Australian rainy season there is also a consequent increasing linear trend in the accumulated seasonal rainfall, which displays a slope of 2.85 mm yr^{-1} (Fig. 2d). However, it is not obvious if this linear trend in seasonal accumulation of rainfall in Fig. 2d is a result of the increasing length of the season or a result of an increasing daily rain rate or a combination of both. To resolve this issue, we examined the time series of the seasonal rain in units of daily rain rate in Fig. 2e and found a similar increasing trend of 0.01 mm day^{-1} yr^{-1}. This result in Fig. 2e clearly suggests that the northern Australian rainy season has an increasing trend of the seasonal accumulation of rain from a combination of both increasing length of the season and an increasing mean daily rain rate.

A concern with long-term analyzed datasets such as the precipitation analysis used in this work is that the density of observing stations vary with time, which can introduce artificial trends. Jones et al. (2009) indicate that the density of rain gauge stations contributing to the rainfall analysis over Australia vary from just over 3000 to well over 6000 in 2010. This is one of the reasons that we developed the rainfall index by area averaging over a large area like northern Australia (Fig. 1a). Further, to allay this concern we examined the trends of the seasonal rainfall over the Darwin airport station in northern Australia, which had longest uninterrupted observations of daily rainfall from 1941 to 2020. We performed the analysis on this station data similar to that in Fig. 2 and

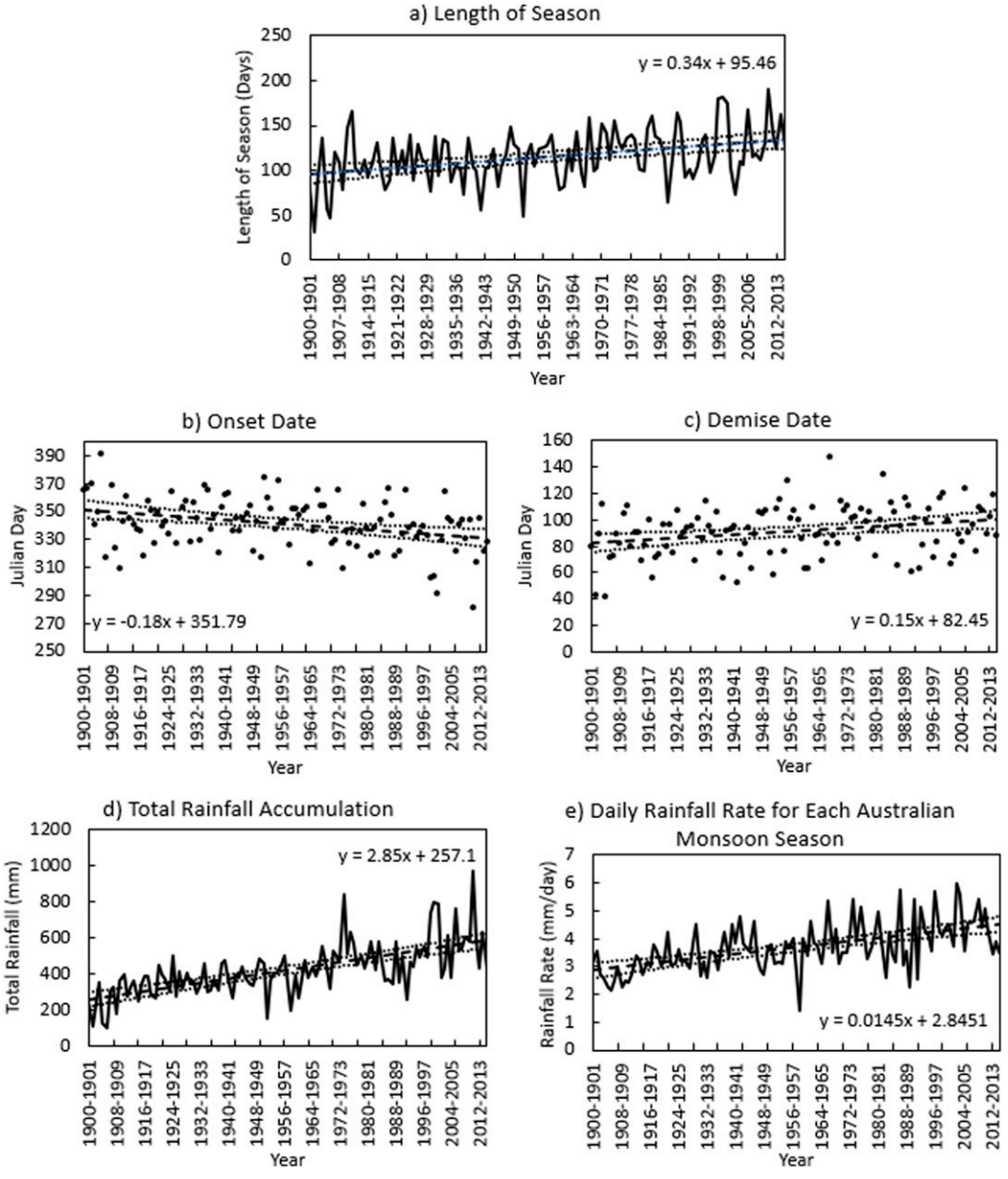

FIG. 2. (a) Length (days), (b) onset (Julian) day, (c) demise (Julian) day, (d) seasonal accumulation of rainfall (mm), and (e) mean seasonal rain rate (mm day^{-1}) of the northern Australian rainy season. The least squares fit line (dashed line) is overlaid with the 95% confidence interval (dotted lines). The slope of the regression line is indicated in each panel with appropriate units.

found that similar trends were observed as with the aggregated data over northern Australia (not shown). This further confirmed that the trends seen in Fig. 2 are not an artifact of the changing density of observations in the region.

It may be noted that many earlier studies have also indicated a rising trend in the daily rain rates over northern Australia during the wet season (e.g., Suppiah and Hennessy 1996, 1998; Smith 2004; Nicholls and Collins 2006; Taschetto and England 2009; Catto et al. 2012; Gallego et al. 2017; Dey et al. 2019; Hassim and Timbal 2019). Taschetto and England (2009) attributed the trend to corresponding changes in the tropical Pacific and Indian Ocean SST. Catto et al. (2012) find that the rising trend in the summer rainfall over northern Australia is a result of corresponding circulation changes occurring during the buildup and the demise of the monsoon season in which the low-level northeasterly

TABLE 2. Sen slope and z-score values for Mann–Kendall test of linear trends shown in Fig. 2. The scores are calculated for $\alpha = 0.01$.

	Sen slope	z-score
Length of season	0.3	3.86
Onset	−0.2	−2.78
Demise	0.2	2.68
Seasonal rainfall accumulation	2.6	7.80
Seasonal rainfall rate	0.01	6.41

flow transports moist air into the northern Australia region, which result in the lengthening of the season. This is consistent with the diagnosis of earlier onset and later onset of the rainy season shown in Fig. 2. Furthermore, we also find, consistent with the reported observations of Catto et al. (2012), a trend of stronger easterly anomalies at 850 hPa on the day of the onset and demise (not shown). Some studies have suggested that some of these changes in circulation over northern Australia stem from increased aerosol emissions (Rotstayn et al. 2012), while Lin and Li (2012) argue that they are manifestations of the remote impact of warming in the tropical Atlantic.

b. *Seasonal evolution of the rainy season*

In this subsection we will relate the evolution of the rainy season over northern Australia as defined in this paper with the more familiar seasonal evolution of the Australian summer monsoon. The similarity in the two seasons are quite apparent given the fact that the annual peak of rainfall over northern Australia is coincident in both seasons.

A composite of the daily area-averaged rainfall over northern Australia was calculated for the period from 30 days prior to 30 days after the onset date of each rainy season. Figure 3 shows the composite spatial distribution of rainfall over northern Australia (in mm) for 30, 25, 20, 15, 10, and 5 days and for 1 day prior to the onset, and for the day of the onset, as well as for 1 day and 5, 10, 15, 20, 25, and 30 days after the onset of the rainy season. These composites show the gradual appearance of stronger precipitation rates over northern Australia as the day of onset is approached. For example, days before the onset of the rainy season the rain rate is around 1–4 mm day^{-1} over northern Australia. On the day of the onset and thereafter, rain rates exceeding 9 mm day^{-1} are observed over northern Australia (Fig. 3).

The same type of composite of the daily rainfall is created around the demise date of the Australian rainy season in Fig. 4. The panels in Fig. 4 clearly show that rain rates exceeding 9 mm day^{-1} over major portions of northern Australia persist through the day of demise date of the rainy season. But thereafter the rain rates begin to decline, with regions exceeding a rain rate of 9 mm day^{-1} appearing more sporadic spatially.

Similarly, the evolution of the composite 850-hPa wind, centered around the onset date of the rainy season, is displayed in Fig. 5. The subtropical anticyclonic flow dominates over continental Australia while zonal easterlies are predominant over northern Australia in days prior to the onset. The monsoon trough[1] does not appear over northern Australia (~13°S) until about 15 days after the onset date (Fig. 5). Thereafter, the trough remains at around the same latitude. At the same time, the westerlies begin to gradually accelerate over the Flores Sea around 5 days after the onset date and gradually expand their acceleration poleward and eastward in the subsequent days (Fig. 5). In the meanwhile, the anticyclonic flow over continental Australia becomes weaker and transient in the post-onset period (Fig. 5). It should be noted that the westerlies at 850 hPa do not appear over northern Australia until about 10 days after the onset date (Fig. 5). These differences between the composites of the low-level winds and daily rain rate highlight the differences between our definition of the rainy season and the traditional monsoon season over northern Australia.

Likewise, the monsoon trough begins to gradually move equatorward almost 30 days before the demise date of the rainy season (Fig. 6). By 15 days prior to the demise date, the trough is well north of Australia and easterlies prevail over all of Australia (Fig. 6). Again, this points to the potential lengthening of the rainy season by our definition relative to the traditional monsoon season over northern Australia that is based on changes in wind circulation. The zonal easterlies over northern Australia begin to accelerate even 30 days before the demise and continue to accelerate even further in the 30-day period post-demise date (Fig. 6). In the meanwhile, the westerlies, which are confined to the Flores and the Banda Sea region, begin to decelerate from around 30 days before the demise date.

A heuristic model of the monsoons it that it is a giant sea breeze driven by a hot land surface and relatively cool surrounding ocean (Murakami and Nakazawa 1985; Kawamura et al. 2002; Hung and Yanai 2004; Hendon 2005). The basis for such an analogy to the sea breeze is that the sensible heating over the hot land surface in the pre-monsoon season leads to the reversal of the temperature gradient that leads to the onshore monsoon flow (Hendon 2005). The evolution of the surface

[1] The monsoon trough in Figs. 5 and 6 is drawn along the axis of minimum wind speed and marking the boundary between reversal of wind direction.

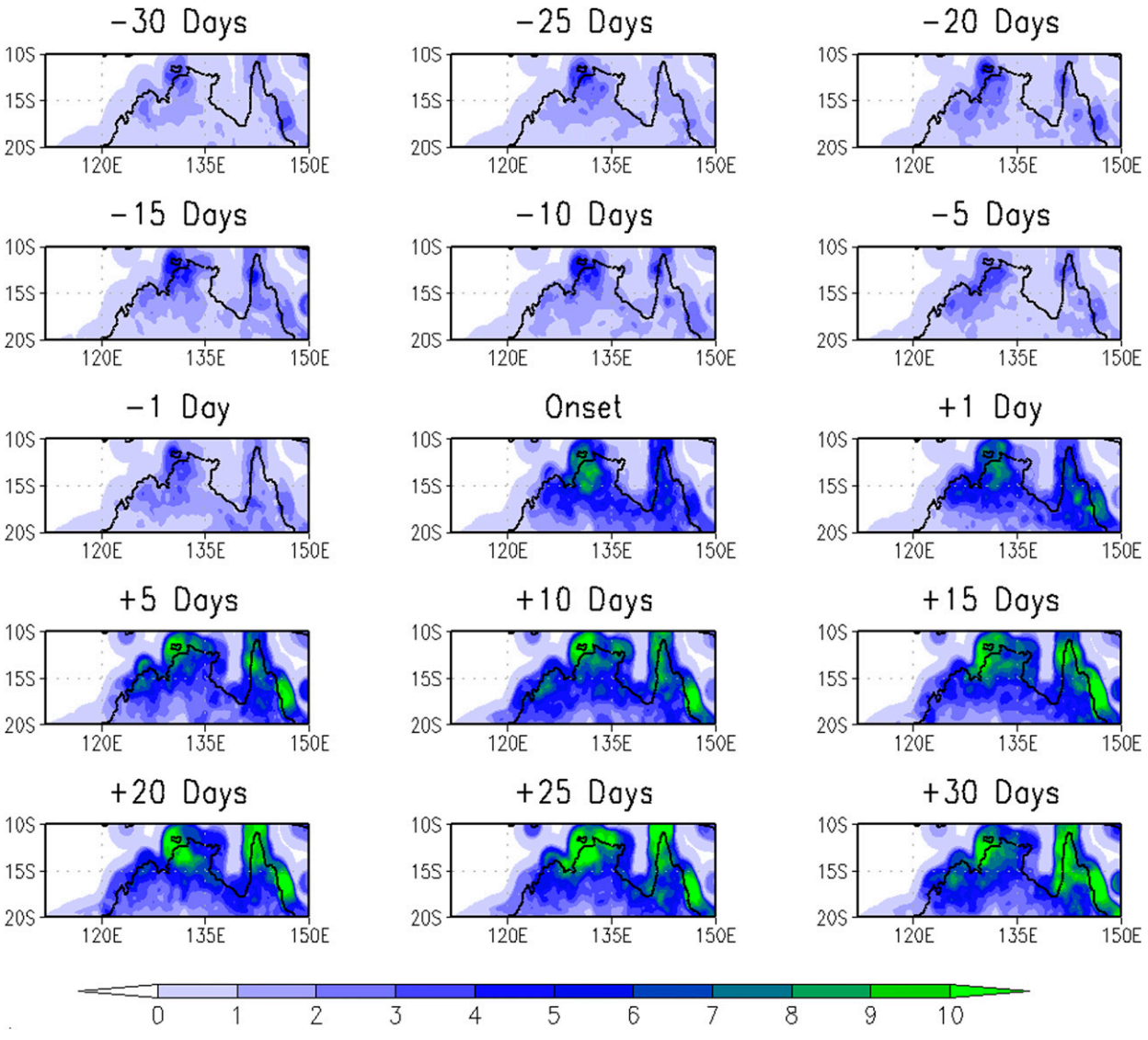

FIG. 3. The composite spatial distribution of rainfall (mm day^{-1}) over northern Australia for 30, 25, 20, 15, 10, and 5 days and 1 day prior to onset date and for the day of the onset of the Australian rainy season, as well as the composite spatial distribution of rainfall for 1 day and 5, 10, 15, 20, 25, and 30 days after the onset of the rainy season, computed over the period from 1900 to 2015.

temperature in Fig. 7 suggests the warming of the land surface over continental Australia continues until the day of the onset and thereafter begins to cool while maintaining the warm land and cold ocean contrast in the post-onset period of the evolution of the monsoon. It is interesting to note that the temperature contrast between the land surface and the ocean is strongest about 5 days before the onset of the rainy season and thereafter it begins to reduce until about 1 day post-onset of the rainy season (Fig. 7). Subsequently, the northern Australian region remains cool relative to the onset-date temperature but the arid central Australian region remains comparatively warm and maintains the land–ocean thermal contrast. Similarly, the composite evolution of surface temperature around the demise date of the rainy season in Fig. 8 shows that while the contrast of the warm land and cold ocean is maintained prior to the demise date, in the post-demise period this contrast decreases with the land surface across continental Australia cooling significantly. The oceans surrounding Australia also begin to cool relative to the demise date of the northern Australian rainy season (Fig. 8).

As noted, our definition of the rainy season tends to be longer than the Australian monsoon season. The monsoon's iconic features of low-level westerlies and monsoon trough appear later and retreat earlier than the

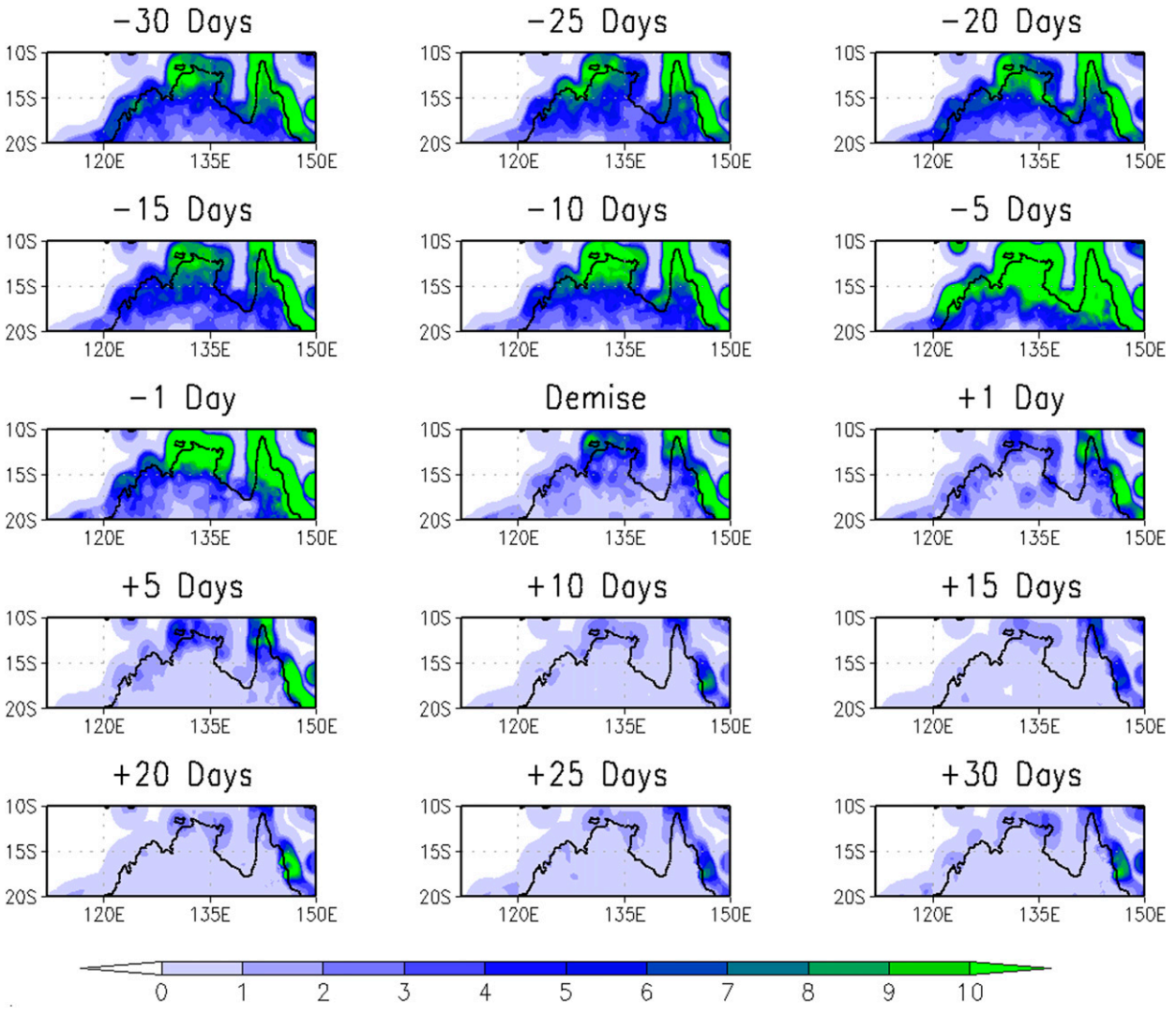

FIG. 4. The composite spatial distribution of rainfall (mm day^{-1}) over northern Australia for 30, 25, 20, 15, 10, and 5 days and 1 day prior to the demise date and for the day of the demise of the Australian rainy season, as well as the average spatial distribution of rainfall for 1 day and 5, 10, 15, 20, 25, and 30 days after the demise of the rainy season, computed over the period from 1900 to 2015.

onset and demise of the rainy season. Some of the earlier definitions of the onset/demise of the Australian monsoon season were based on wind anomalies (e.g., Troup 1961, Holland 1986, Kajikawa et al. 2010). But as Davidson et al. (1983) indicate, the monsoon rains usually follow the mass convergence of the winds by a few days. Therefore, there is a tendency for the wind-based onset dates to be earlier than the rain-based onset dates. The mean absolute difference of our diagnosed onset dates with the 14 other onset dates compared in Fig. 3 of Lisonbee et al. (2020) that are classified as those based on rainfall only (four indices), wind only (five indices), a combination of wind and rain (two indices), and other parameters (three indices) ranges from 4 to 34.5, 0.5 to 23, 0.5 to 24.5, and 0.4 to 41 mm day^{-1}, respectively.

c. *Interannual variability*

Noska and Misra (2016) and Misra et al. (2017) note that one of the advantages of diagnosing the onset date of the Indian monsoon is that its variations are also closely associated with the variations of the length of the monsoon season and the seasonal rainfall anomalies. Therefore, it is possible to leverage this relationship by monitoring the onset date of the Indian monsoon to provide an outlook of the evolution of the rest of the monsoon season (Bhardwaj and Misra 2019). The correlations in Table 3 suggest that an early or later onset

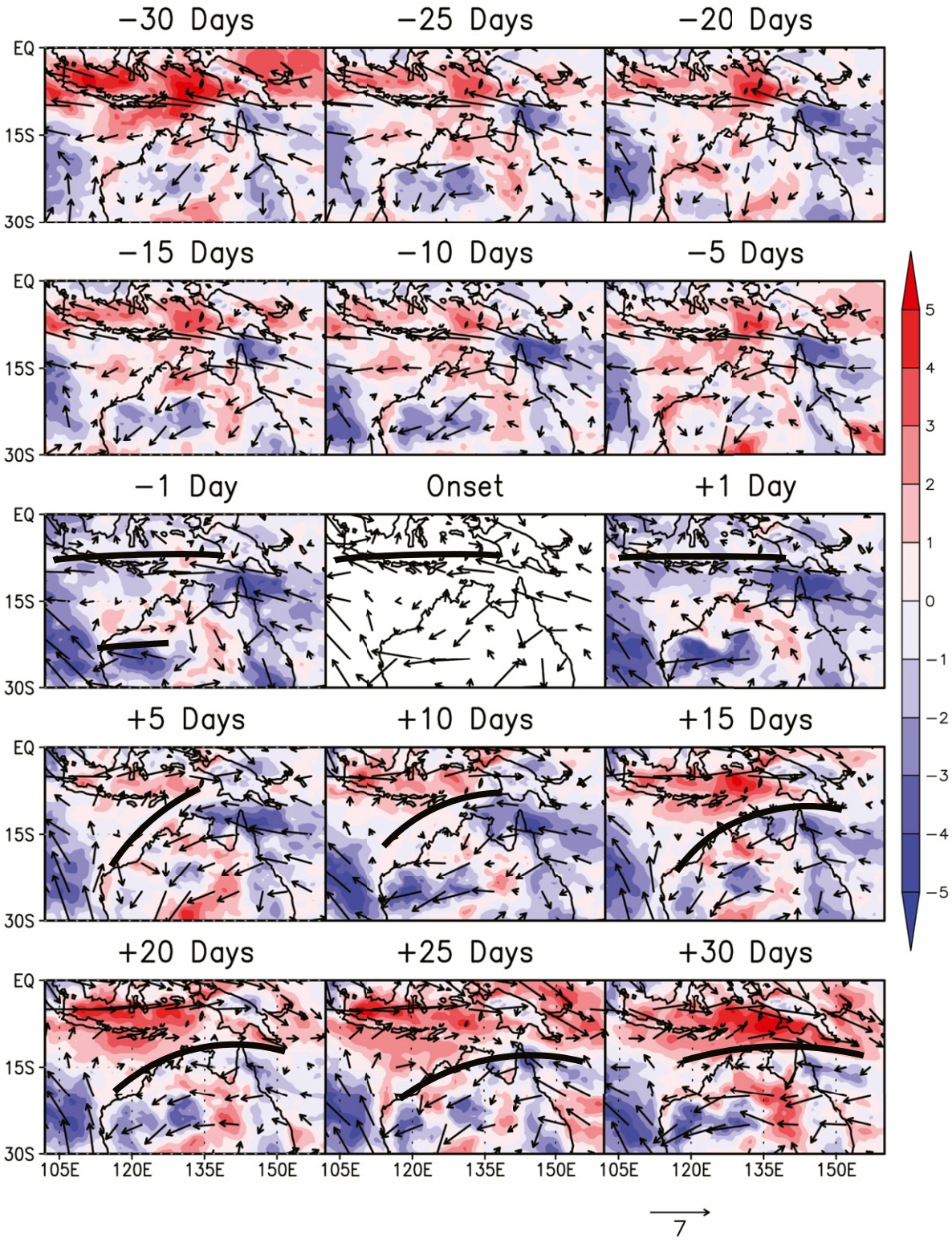

FIG. 5. The composite of the 850-hPa winds (m s^{-1}; vectors) over the Australian region for 30, 25, 20, 15, 10, and 5 days and 1 day before the onset and for +1, +5, +10, +15, +20, +25, and +30 days after the onset date of the rainy season. The wind speed anomalies are shaded (see color bar), with the anomalies computed as the composite difference from the onset date. The black thick line in some panels represents the trough axis, which is based on the corresponding composite total wind field.

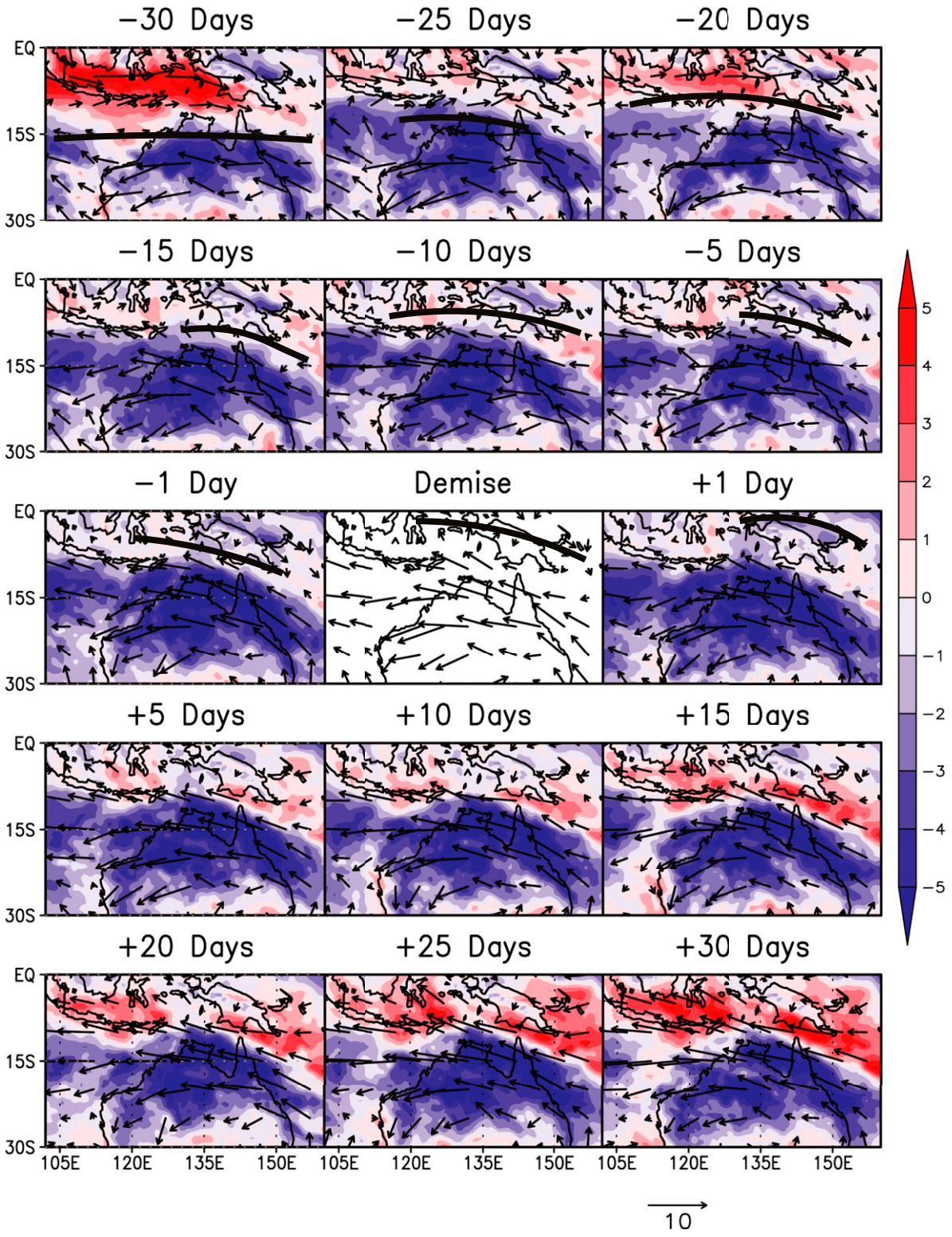

FIG. 6. The composite of the 850-hPa winds (m s^{-1}; vectors) over the Australian region for 30, 25, 20, 15, 10, and 5 days and 1 day before the demise and for +1, +5, +10, +15, +20, +25, and +30 days after the demise date of the rainy season. The wind speed anomalies are shaded (see color bar), with the anomalies computed as the composite difference from the onset date. The black thick line in some panels represents the trough axis, which is based on the corresponding composite total wind field.

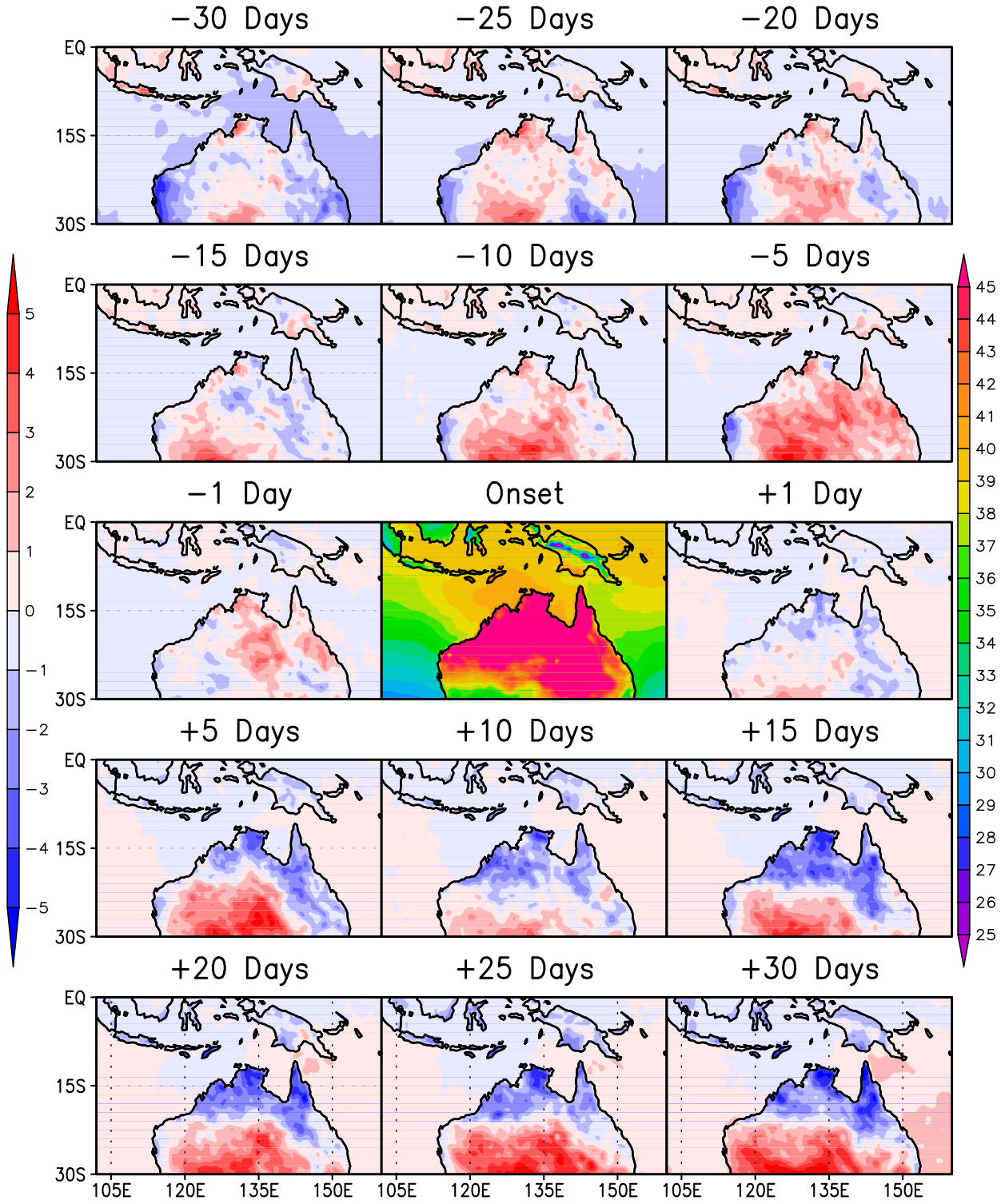

FIG. 7. The composite spatial distribution of the land surface temperature and SST anomalies (°C) over the Australian region for 30, 25, 20, 15, 10, and 5 days and 1 day prior to the onset of the northern Australian rainy season. Also shown are the composite land surface temperature and SST anomalies (°C) for 1 day and 5, 10, 15, 20, 25, and 30 days after the onset of the rainy season over the period from 1900 to 2015. The anomalies are computed based on the difference from the onset date SST and land surface temperature. The full field of the SST and land surface temperature are shown for the date of the onset of the rainy season with its color bar on the right. The color bar for the anomalies is on the left.

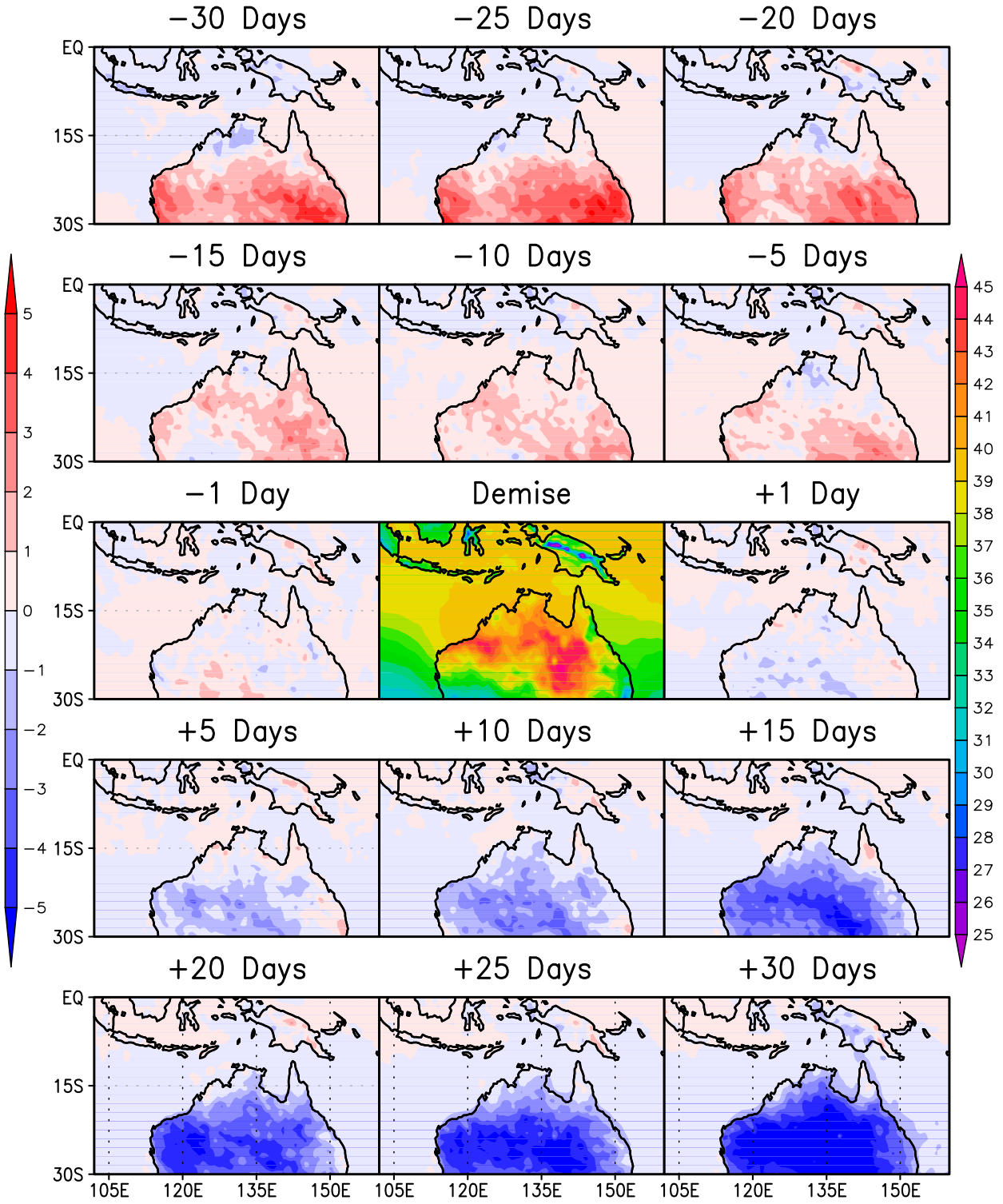

FIG. 8. The composite spatial distribution of the land surface temperature and SST anomalies (°C) over the Australian region for 30, 25, 20, 15, 10, and 5 days and 1 day prior to the demise of the northern Australian rainy season. Also shown are the composite land surface temperature and SST anomalies (°C) for 1 day and 5, 10, 15, 20, 25, and 30 days after the demise of the rainy season over the period from 1900 to 2015. The anomalies are computed based on the difference from the demise date SST and land surface temperature. The full field of the SST and land surface temperature are shown for the date of the demise of the rainy season with its color bar on the right. The color bar for the anomalies is on the left.

TABLE 3. Correlations of the parameters of the Australian rainy season. The values with single and double asterisks are significant at 95% and 99% confidence interval according to a *t* test, respectively. The trends were removed in all the variables before the correlations were performed.

	Onset	Demise	Length	Seasonal rainfall anomaly	Seasonal surface temperature anomaly
Onset	1.00	−0.18	−0.75**	−0.65**	0.47**
Demise	−0.18	1.00	0.79**	0.41**	−0.22*
Length	−0.75**	0.79**	1.00	0.68**	−0.45**
Seasonal rainfall anomaly	−0.65**	0.41**	0.68**	1.00	−0.55**
Seasonal surface temperature anomaly	0.47**	−0.22**	−0.45**	−0.55**	1.00

date of the rainy season is associated with longer or shorter length of the season, wetter or drier, and colder or warmer northern Australian rainy season, respectively. Similarly, Table 3 indicates that early or later retreat date of the rainy season is associated with shorter or longer length of the season, drier or wetter, and colder or warmer northern Australian wet season, respectively. A partial correlation analysis [see Eq. (3) below] reveals that the onset date variations have a stronger bearing on the seasonal anomalies of rainfall and temperature of the northern Australian rainy season compared to the demise date variations (Table 4). It may be noted however that the bearing of the onset and demise date variations on the length of the northern Australian rainy season is comparable (Table 4).

The partial correlation is given by

$$r_{ab/c} = \frac{[r_{ab} - r_{ac}r_{bc}]}{\sqrt{1 - r_{ac}^2}\sqrt{1 - r_{bc}^2}}, \tag{3}$$

where $r_{ab/c}$ is the correlation between two variables a and b after removing the influence of c on a and b. Similarly, r_{ab}, r_{ac}, and r_{bc} are correlations between variables a and b, a and c, and b and c, respectively.

ENSO is one of the most important external influences on the interannual variations of the Australian monsoon (Holland 1986; McBride 1987; Suppiah 1992)

TABLE 4. Partial correlations to determine the relative influence of onset and retreat date variations on the seasonal rainfall, surface temperature, and length anomalies of the Australian rainy season. Double asterisks indicate that values are significant at 99% confidence interval according to a *t* test.

	Seasonal rainfall	Seasonal surface temperature	Seasonal length
Onset date	−0.65**	0.37**	−0.998**
Retreat date	0.42**	−0.09	0.998**

and therefore we have explored its influence on the characteristics of the northern Australian rainy season. The scatterplot of the September through November (SON) mean Niño-3.4 sea surface temperature anomalies (used as a proxy for ENSO index and obtained from the corresponding SST data from CFSR) versus the onset day of the rainy season in Fig. 9a indicates an R^2 value of 0.27, which is significant at 95% confidence interval (according to a *t* test). This relationship in Fig. 9a suggests that warm or cold ENSO events in the SON season is associated with a greater likelihood of the northern Australian rainy season onset to be later or earlier than normal, respectively. However, the relationship between the retreat date of the rainy season and the ENSO index in Fig. 9b is relatively weak (and statistically insignificant). But the scatter between the ENSO index and the length of the northern Australian rainy season (Fig. 9c; which shows statistically significant correlation at 95% confidence interval with $R^2 = 0.25$) shows that warm or cold ENSO events in the SON season are more likely to relate to a short or long northern Australian rainy season, respectively. The northern Australian rainy season precipitation anomalies (in mm) show a strong linear relationship with the SON ENSO index (Figs. 9d,e). The rainfall accumulation anomalies over the fixed December–February (DJF) Australian monsoon season indicate below- or above-normal values is associated with warm or cold ENSO anomalies (Fig. 9d). Similarly, Fig. 9e suggests that the variable northern Australian rainy season is likely to be drier or wetter in warm or cold ENSO years, respectively. It may be noted, however, that the relationship of the ENSO anomalies with the northern Australian seasonal rainfall becomes stronger when variations in the length of the rainy season is accounted (Fig. 9e) compared to the fixed DJF season (Fig. 9d). Additionally, the relationship of the northern Australian rainy seasonal precipitation expressed in rain rates (e.g., mm day^{-1}) with ENSO becomes weaker (not shown). This is because the numerator and the

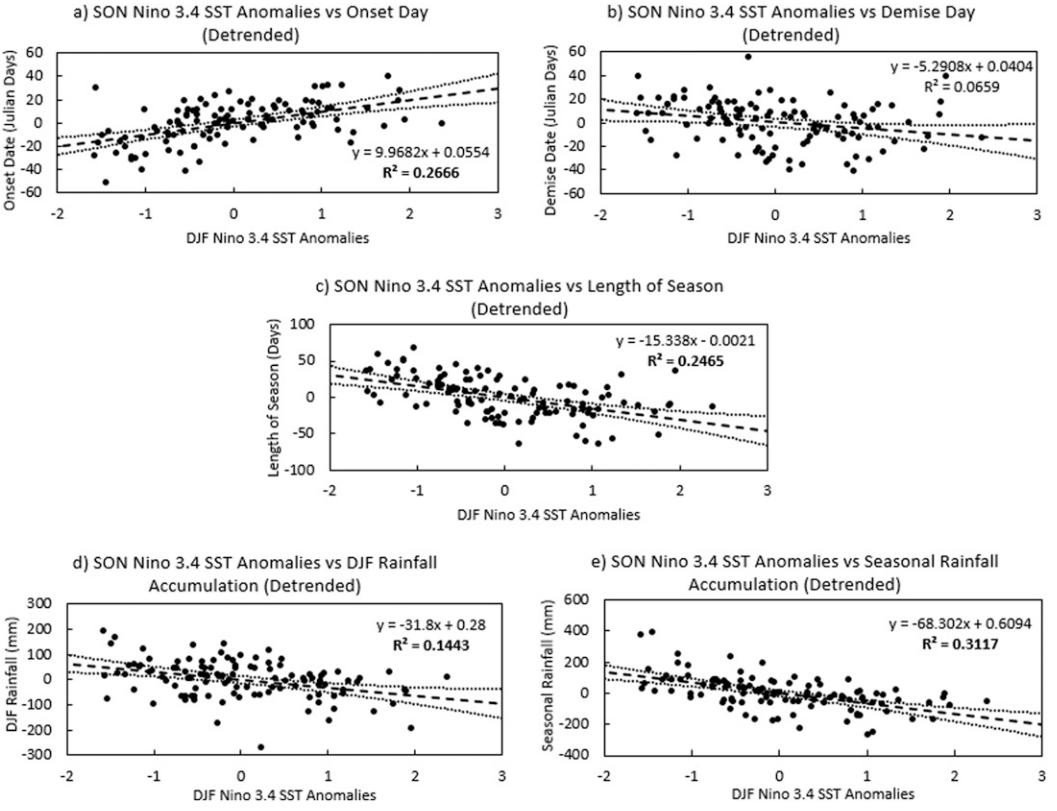

FIG. 9. The scatterplot of the September–November-averaged Niño-3.4 sea surface temperature anomalies with anomalies of (a) onset date, (b) demise date, (c) length of the season (days), (d) DJF rainfall accumulation (mm), and (e) seasonal rainfall accumulation (mm) with varying seasonal length of the Australian rainy season. All panels are overlaid with the least squares fit line (dashed line) of the data along with the 95% confidence interval (dotted lines). The R^2 value is shown in each panel and is boldface if it is significant at 95% confidence interval according to a *t* test. All variables are detrended beforehand.

denominator of the mean seasonal rain rate (=seasonal accumulation of rainfall/length of the season) vary in compensatory manner during anomalous ENSO years to yield very weak anomalies of the seasonal rain rate.

The compelling reason for the improved relationship of the seasonal rainfall anomalies that accounts for varying seasonal length with the ENSO index follows from Hendon et al. (2002), who noted the strong ENSO influence on the pre-monsoon seasonal rainfall in the late austral spring season. Our results are consistent with this finding as the onset date variations show the enhanced teleconnectivity with ENSO compared to the demise date variations (Fig. 9). Although this pre-monsoon rainfall over northern Australia is usually far less intense than during the monsoon season, it is found to be critical for agriculture in the region and is far more predictable by both statistical and dynamical models (Hendon et al. 2002). Hendon et al. (2002) subscribe this enhanced predictability of the pre-monsoon rainfall from local air–sea interaction that enhances the teleconnection with ENSO while the same local air–sea interaction begins to deteriorate the predictability during the monsoon season.

5. Conclusions

The definition of the onset and demise of the Australian rainy season proposed in this paper is a robust and comprehensive index that is objectively determined. We make a subtle distinction between the Australian rainy season and the Australian monsoon season as our definition does not meet the ''traditional'' definition of the monsoon, which seeks the arrival of the westerlies over northern Australia for the onset of the monsoon. Likewise, the equatorward retreat of the trough at the demise of the season is not sought in our proposed definition of the season. The definition of the season as introduced in this paper is solely based on daily rainfall rates and is therefore appropriately defining the rainy season. However, the rainy season as

defined in the paper significantly overlaps to a large extent with the monsoon season.

This proposed definition of the rainy season over northern Australia distinguishes itself from other indices of the Australian monsoon introduced in earlier studies. For example, Wang et al. (2004) defined an Australian monsoon index based on the 850-hPa winds. Likewise, Kajikawa et al. (2010) defined a similar monsoon index. Webster (2006) introduced a vertical shear index between 850 and 200 hPa over northern Australia to define the Australian monsoon season. However, as we found in the discussion of Fig. 5 the wind shift in the low levels does not happen until well over 10 days after the diagnosis of the onset date of the rainy season from the proposed methodology in the paper. Similarly, the wind shift over northern Australia happens much earlier than the diagnosis of the demise date of the rainy season (Fig. 6). In other words, the proposed definition of the onset/demise date of the rainy season in this paper differs from the wind-based indices of the Australian monsoon, which depend on the seasonal shift of the low-level winds. Furthermore, because our definition offers the diagnosis of the onset/demise of the rainy season to a specific date of the year, the variations in the length of the rainy season can be accounted for. This is unique to our definition of the season relative to other monsoon season indices that used fixed seasonal (DJF) average (Wang et al. 2004; Webster 2006; Kajikawa et al. 2010).

There is a significant linear trend that manifest with a rising rate of the length of the Australian rainy season of 0.34 days yr^{-1}. This is due to a linear trend in the onset date of the season, which is occurring earlier at the rate of 0.18 days yr^{-1}, and a linear trend in the retreat date that shows it is occurring later at the rate of 0.15 days yr^{-1}. On account of these changes in the evolution of the Australian monsoon, there is also an increasing trend in the seasonal accumulation of rain from a combination of both increasing length of the season and an increasing mean daily rain rate. Although we have not attempted to understand the mechanism for these observed trends, it is consistent with some of the earlier findings of Catto et al. (2012) that suggest a trend of stronger moist easterlies at 850 hPa around the onset and demise of the season that is attributed as a cause for the trend of longer wet seasons over northern Australia.

Analysis of the interannual variations of the Australian rainy season suggests that early onset of the season results in a longer, wetter, and colder season. Likewise, later onset of the season results in a shorter, drier, and warmer season. Similarly, early retreat (which is independent of the onset date variations) of the rainy season also causes a shorter, drier, and warmer season. Likewise, later retreat of the season is associated with a longer, wetter, and colder season. However, the influence of the onset date variations on the seasonal rain and surface temperature anomalies dominates compared to the demise date variations. These relationships with the onset date of the season are important and could be leveraged effectively to provide an outlook for the evolution of the ensuing rainy season as demonstrated in Bhardwaj and Misra (2019) with regard to the Indian summer monsoon. The ENSO variations also affect the seasonal length and rainfall anomalies of the Australian rainy season. Our definition of the Australian rainy season that accounts for the varying length of the season amplifies the teleconnection of ENSO with the seasonal rainfall anomalies compared to the fixed calendar month (DJF) Australian seasonal rainfall anomalies.

Our proposed indices for the northern Australian rainy season is easily adaptable for operational applications and is not limited in spatial scale to any specific region of northern Australia. These are limitations that Lisonbee et al. (2020) recognized in many of the current indices for understanding the Australian monsoon or wet season variations.

Acknowledgments. We thank the Australian Bureau of Meteorology for providing the rainfall dataset and acknowledge https://climatedataguide.ucar.edu/climate-data/climate-forecast-system-reanalysis-cfsr for the reanalysis dataset used in the paper. This work was supported by NASA Grants NNX17AG72G and NNX16AD83G and NSF Award 1606296.

REFERENCES

Anwar, M. R., G. O'Leary, D. McNeil, H. Hossain, and R. Nelson, 2007: Climate change impact on rainfed wheat in south-eastern Australia. *Field Crops Res.*, **104**, 139–147, https://doi.org/10.1016/j.fcr.2007.03.020.

Atkinson, G. D., 1971: Forecasters' guide to tropical meteorology. Air Weather Service (MAC), United States Air Force Tech. Rep. 240, 360 pp.

Bhardwaj, A., and V. Misra, 2019: Monitoring the Indian summer monsoon evolution at the granularity of the Indian Meteorological sub-divisions using remotely sensed rainfall products. *Remote Sens.*, **11**, 1080, https://doi.org/10.3390/rs11091080.

Catto, J. L., C. Jakob, and N. Nicholls, 2012: The influence of changes in synoptic regimes on north Australian wet season rainfall trends. *J. Geophys. Res.*, **117**, D10102, https://doi.org/10.1029/2012JD017472.

Cook, G. D., and R. G. Heerdegen, 2001: Spatial variation in the duration of the rainy season in monsoonal Australia. *Int. J. Climatol.*, **21**, 1723–1732, https://doi.org/10.1002/joc.704.

Davidson, N. E., J. L. McBride, and B. J. McAvaney, 1983: The onset of the Australian monsoon during winter MONEX: Synoptic aspects. *Mon. Wea. Rev.*, **111**, 496–516, https://doi.org/10.1175/1520-0493(1983)111<0496:TOOTAM>2.0.CO;2.

——, ——, and ——, 1984: Divergent circulations during the onset of the 1978–79 Australian monsoon. *Mon. Wea. Rev.*, **112**, 1684–1696, https://doi.org/10.1175/1520-0493(1984)112<1684:DCDTOO>2.0.CO;2.

Dey, R., S. C. Lewis, J. M. Arblaster, and N. J. Abram, 2019: A review of past and projected changes in Australia's rainfall. *Wiley Interdiscip. Rev.: Climate Change*, **10**, e00577, https://doi.org/10.1002/WCC.577.

Drosdowsky, W., 1996: Variability of the Australian summer monsoon at Darwin: 1957–1992. *J. Climate*, **9**, 85–96, https://doi.org/10.1175/1520-0442(1996)009<0085:VOTASM>2.0.CO;2.

Gallego, D., R. Garcia-Herrera, C. Peña-Ortiz, and P. Ribera, 2017: The steady enhancement of the Australian summer monsoon in the last 200 years. *Sci. Rep.*, **7**, 16166, https://doi.org/10.1038/S41598-017-16414-1.

Grant, I., 2012: Daily rain gauge precipitation (rainfall)–Gridded, Australia coverage, accessed July 2017, http://data.auscover.org.au/xwiki/bin/view/Product+pages/Product+User+Page+Melbourne+2.

Hassim, M. E. E., and B. Timbal, 2019: Observed rainfall trends over Singapore and the Maritime Continent from the perspective of regional-scale weather regimes. *J. Appl. Meteor. Climatol.*, **58**, 365–384, https://doi.org/10.1175/JAMC-D-18-0136.1.

Hendon, H., 2005: The Australian summer monsoon. The Global Monsoon System: Research and Forecast, Rep. of the Int. Committee of the Third Int. Workshop on Monsoons (IWM-III), WMO/TD 1266, Geneva, Switzerland, WMO, 179–196.

——, E. Lim, and M. C. Wheeler, 2002: Seasonal prediction of Australian summer monsoon rainfall. *The Global Monsoon System, Research and Forecast*, 2nd ed., C. P. Chang et al., Eds., World Scientific, 73–83, https://doi.org/10.1142/9789814343411_0005.

Hirsch, R. M., and J. R. Slack, 1984: A nonparametric trend test for seasonal data with serial dependence. *Water Resour. Res.*, **20**, 727–732, https://doi.org/10.1029/WR020i006p00727.

Holland, G. J., 1986: Interannual variability of the Australian summer monsoon at Darwin: 1952–82. *Mon. Wea. Rev.*, **114**, 594–604, https://doi.org/10.1175/1520-0493(1986)114<0594:IVOTAS>2.0.CO;2.

Hung, C.-W., and M. Yanai, 2004: Factors contributing to the onset of the Australian summer monsoon. *Quart. J. Roy. Meteor. Soc.*, **130**, 739–758, https://doi.org/10.1256/qj.02.191.

Jones, D. A., W. Wang, and R. Fawcett, 2009: High-quality spatial climate datasets for Australia. *Aust. Meteor. Oceanogr. J.*, **58**, 233–248, https://doi.org/10.22499/2.5804.003.

Kajikawa, Y., B. Wang, and J. Yang, 2010: A multi-time scale Australian monsoon index. *Int. J. Climatol.*, **30**, 1114–1120, https://doi.org/10.1002/joc.1955.

Kawamura, R., Y. Fukuta, H. Ueda, T. Matsuura, and S. Lizuka, 2002: A mechanism of the onset of the Australian summer monsoon. *J. Geophys. Res.*, **107**, 4204, https://doi.org/10.1029/2001JD001070.

Liebmann, B., S. J. Camargo, A. Seth, J. A. Marengo, L. M. V. Carvalho, D. Allured, R. Fu, and C. S. Vera, 2007: Onset and end of the rainy season in South America in observations and the ECHAM 4.5 atmospheric general circulation model. *J. Climate*, **20**, 2037–2050, https://doi.org/10.1175/JCLI4122.1.

Lin, Z., and Y. Li, 2012: Remote influence of the tropical Atlantic on the variability and trend in North West Australia summer rainfall. *J. Climate*, **25**, 2408–2420, https://doi.org/10.1175/JCLI-D-11-00020.1.

Lisonbee, J., J. Ribbe, and M. Wheeler, 2020: Defining the north Australian monsoon onset: A systematic review. *Prog. Phys. Geogr.*, **44**, 398–418, https://doi.org/10.1177/0309133319881107.

Lo, F., and M. C. Wheeler, 2007: Probabilistic forecasts of the onset of the north Australian wet season. *Mon. Wea. Rev.*, **135**, 3506–3520, https://doi.org/10.1175/MWR3473.1.

McBride, J. L., 1983: Satellite observations of the Southern Hemisphere monsoon during winter MONEX. *Tellus*, **35A**, 189–197, https://doi.org/10.1111/j.1600-0870.1983.tb00196.x.

——, 1987: The Australian summer monsoon. *Reviews of Monsoon Meteorology*, C. P. Chang and T. N. Krishnamurti, Eds., Oxford University Press, 203–231.

Misra, V., A. Mishra, and A. Bhardwaj, 2017: Local onset and demise of the Indian summer monsoon. *Climate Dyn.*, **51**, 1609–1622, https://doi.org/10.1007/s00382-017-3924-2.

Murakami, T., and A. Sumi, 1982: Southern Hemisphere summer monsoon circulation during the 1978–79 WMONEX. Part I: Monthly mean wind fields. *J. Meteor. Soc. Japan*, **60**, 638–648, https://doi.org/10.2151/jmsj1965.60.2_638.

——, and T. Nakazawa, 1985: Transition from the Southern to Northern Hemisphere summer monsoon. *Mon. Wea. Rev.*, **113**, 1470–1486, https://doi.org/10.1175/1520-0493(1985)113<1470:TFTSTN>2.0.CO;2.

——, and J. Matsumoto, 1994: Summer monsoon over the Asian continent and western North Pacific. *J. Meteor. Soc. Japan*, **72**, 719–745, https://doi.org/10.2151/jmsj1965.72.5_719.

Nicholls, N., 1984: A system for predicting the onset of the north Australian wet season. *J. Climatol.*, **4**, 425–435, https://doi.org/10.1002/joc.3370040407.

——, and D. Collins, 2006: Observed climate change in Australia over the past century. *Energy Environ.*, **17**, 1–12, https://doi.org/10.1260/095830506776318804.

——, J. L. McBride, and R. J. Ormerod, 1982: On predicting the onset of the Australian wet season at Darwin. *Mon. Wea. Rev.*, **110**, 14–17, https://doi.org/10.1175/1520-0493(1982)110<0014:OPTOOT>2.0.CO;2.

Noska, R., and V. Misra, 2016: Characterizing the onset and demise of the Indian summer monsoon. *Geophys. Res. Lett.*, **43**, 4547–4554, https://doi.org/10.1002/2016GL068409.

Qureshi, M. E., M. A. Hanjra, and J. Ward, 2013: Impact of water scarcity in Australia on global food security in an era of climate change. *Food Policy*, **38**, 136–145, https://doi.org/10.1016/j.foodpol.2012.11.003.

Rotstayn, L. D., S. J. Jeffrey, M. A. Collier, S. M. Dravitzki, A. C. Hirst, J. I. Syktus, and K. K. Wong, 2012: Aerosol- and greenhouse gas-induced changes in summer rainfall and circulation in the Australasian region: A study using single-forcing climate simulations. *Atmos. Chem. Phys.*, **12**, 6377–6404, https://doi.org/10.5194/acp-12-6377-2012.

Saha, S., and Coauthors, 2010: The NCEP Climate Forecast System Reanalysis. *Bull. Amer. Meteor. Soc.*, **91**, 1015–1057, https://doi.org/10.1175/2010BAMS3001.1.

Sen, P. K., 1968: Estimates of the regression coefficient based on Kendall's tau. *J. Amer. Stat. Assoc.*, **63**, 1379–1389, https://doi.org/10.1080/01621459.1968.10480934.

Smith, I., 2004: An assessment of recent trends in Australian rainfall. *Aust. Meteor. Mag.*, **53**, 163–173.

Smith, I. N., L. Wilson, and R. Suppiah, 2008: Characteristics of the northern Australian rainy season. *J. Climate*, **21**, 4298–4311, https://doi.org/10.1175/2008JCLI2109.1.

Suppiah, R., 1992: The Australian summer monsoon: A review. *Prog. Phys. Geogr.*, **16**, 283–318, https://doi.org/10.1177/030913339201600302.

——, and K. J. Hennessy, 1996: Trends in the intensity and frequency of heavy rainfall in tropical Australia and links with the Southern Oscillation. *Aust. Meteor. Mag.*, **45**, 1–17.

——, and ——, 1998: Trends in total rainfall, heavy rain events and number of dry days in Australia, 1910–1990. *Int. J. Climatol.*, **18**, 1141–1164, https://doi.org/10.1002/(SICI)1097-0088(199808)18:10<1141::AID-JOC286>3.0.CO;2-P.

Tanaka, M., 1994: The onset and retreat dates of the austral summer monsoon over Indonesia, Australia and New Guinea. *J. Meteor. Soc. Japan*, **72**, 255–267, https://doi.org/10.2151/jmsj1965.72.2_255.

Taschetto, A. S., and M. H. England, 2009: An analysis of late twentieth century trends in Australian rainfall. *Int. J. Climatol.*, **29**, 791–807, https://doi.org/10.1002/joc.1736.

Troup, A. J., 1961: Variations in upper tropospheric flow associated with the onset of the Australian monsoon. *Indian J. Meteor. Geophys.*, **12**, 217–230.

Wang, B., R. Wu, and T. Li, 2003: Atmosphere–warm ocean interaction and its impacts on Asian-Australian monsoon variation. *J. Climate*, **16**, 1195–1211, https://doi.org/10.1175/1520-0442(2003)16<1195:AOIAII>2.0.CO;2.

——, L. Ho, Y. Zhang, and M.-M. Lu, 2004: Definition of South China Sea monsoon onset and commencement of the East Asia summer monsoon. *J. Climate*, **17**, 699–710, https://doi.org/10.1175/2932.1.

Webster, P. J., 2006. The coupled monsoon system. *The Asian Monsoon*. B. Wang, Ed., Springer Praxis, 3–66.